

The *PINHEAD/ZWILLE* gene acts pleiotropically in *Arabidopsis* development and has overlapping functions with the *ARGONAUTE1* gene

Karyn Lynn¹, Anita Fernandez², Mitsuhiro Aida³, John Sedbrook², Masao Tasaka³, Patrick Masson² and M. Kathryn Barton^{2,*}

¹Program in Cellular and Molecular Biology and ²Department of Genetics, University of Wisconsin-Madison, Madison, WI 53706, USA

³NARA Institute of Science and Technology, Graduate School of Biological Science, Ikoma Nara 630-0101, Japan

*Author for correspondence (e-mail: mkbarton@facstaff.wisc.edu)

Accepted 10 November 1998; published on WWW 7 January 1999

SUMMARY

Several lines of evidence indicate that the adaxial leaf domain possesses a unique competence to form shoot apical meristems. Factors required for this competence are expected to cause a defect in shoot apical meristem formation when inactivated and to be expressed or active preferentially in the adaxial leaf domain. *PINHEAD*, a member of a family of proteins that includes the translation factor eIF2C, is required for reliable formation of primary and axillary shoot apical meristems. In addition to high-level expression in the vasculature, we find that low-level *PINHEAD* expression defines a novel domain of positional identity in the plant. This domain consists of adaxial leaf primordia and the meristem. These findings suggest that the *PINHEAD* gene product may be a component of a hypothetical meristem forming competence factor. We also

describe defects in floral organ number and shape, as well as aberrant embryo and ovule development associated with *pinhead* mutants, thus elaborating on the role of *PINHEAD* in *Arabidopsis* development. In addition, we find that embryos doubly mutant for *PINHEAD* and *ARGONAUTE1*, a related, ubiquitously expressed family member, fail to progress to bilateral symmetry and do not accumulate the SHOOT MERISTEMLESS protein. Therefore *PINHEAD* and *ARGONAUTE1* together act to allow wild-type growth and gene expression patterns during embryogenesis.

Key words: *Arabidopsis thaliana*, Embryogenesis, Meristem, *PINHEAD*, *ARGONAUTE1*

INTRODUCTION

During embryogenesis, the shoot apical meristem (SAM) arises between the two cotyledons; postembryonically, new SAMs, or axillary meristems, develop in the axils of leaves (the junction between leaf and stem). Thus, SAMs arise in association with leaf-like organs during embryogenesis and later stages of the plant life cycle. The molecular nature and cellular source of signals that direct the formation of a SAM are largely unknown.

Several lines of evidence indicate that the subtending leaf is required for axillary meristem development in dicotyledonous plants. First, in *Arabidopsis*, the axillary bud appears to develop directly on the adaxial leaf base (Talbert et al., 1995). (Adaxial is the side of the leaf toward the long axis of the plant, or the top of the leaf; the abaxial surface faces away from the long axis of the plant, or is the underside of the leaf.) Consistent with this, the bud is clonally related to the subtending leaf (Furner and Pumfrey, 1992; Irish and Sussex, 1992). Second, when the subtending leaf primordium was surgically removed in *Epilobium*, an axillary meristem failed to form (Snow and Snow, 1942).

Additional experiments suggest that the adaxial domain of

the leaf is uniquely competent to form SAMs. Experiments in which cytokinin biosynthetic genes or *KNOTTED*-like homeobox-containing genes were overexpressed resulted in the formation of ectopic meristems (Estruch et al., 1991; Sinha et al., 1993; Chuck et al., 1996). These meristems were limited to adaxial leaf surfaces.

Similarly, cells with adaxial fate were shown to be competent to form SAMs in studies of the *Arabidopsis phabulosa-1d* (*phb-1d*) mutant, in which adaxial leaf fates replace abaxial leaf fates (McConnell and Barton, 1998). In this mutant, meristems are found not only in the expected position on the adaxial leaf base, but also on the adaxialized underside of the leaf. If ectopic meristem formation in *phb-1d* mutants is secondary to the transformation of ab- to adaxial leaf fates, then basal adaxial leaf fate is sufficient for axillary SAM formation.

During embryogenesis, a SAM develops between two cotyledons at their adaxial bases. Thus, the spatial relationship between the SAM and the leaf-like cotyledons is similar to the relationship between the axillary SAM and its subtending leaf. It is possible, therefore, that the adaxial cotyledon domain plays a similar role to that hypothesized for the adaxial leaf domain in promoting SAM formation.

Despite several correlations between adaxial cell fate and meristem formation, the nature of the relationship between them is still unknown. If the adaxial leaf domain is competent to form meristems while other tissues, such as the abaxial leaf domain, do not possess this competence, some factor must exist that is responsible for this unique competence. For example, adaxial cells may express a transcription factor or receptor that allows them to progress through the steps of meristem initiation. We expect such a factor to be expressed or active preferentially in the adaxial side of the leaf and to cause defects in meristem formation when inactivated.

Several genes are required for SAM formation in *Arabidopsis* embryogenesis (reviewed by Evans and Barton, 1997). *SHOOT MERISTEMLESS* (*STM*) is required for SAM initiation and maintenance (Barton and Poethig, 1993; Endrizzi et al., 1996). *STM*, a homeobox-containing gene, is expressed in the presumptive meristem during embryogenesis. Similarly, in the vegetative SAM, *STM* is expressed throughout the meristem except in incipient leaf primordia where its expression is down-regulated.

Mutations in other genes, such as *PINHEAD/ZWILLE* (*PNH*), block SAM development subsequent to initiation. *pnh* mutant embryos form defective SAMs that fail to function as continuous sources of new organs and instead terminate. This is accompanied by the development of a single, central organ (McConnell and Barton, 1995; Moussian et al., 1998). *STM* is expressed in early stages of SAM development in *pnh* embryos but is absent in the terminated meristems (Moussian et al., 1998; Long and Barton, unpublished observations). *pnh* mutants also have reduced frequency of axillary meristem formation (McConnell and Barton, 1995).

Seedlings mutant for either the *REVOLUTA* or the *ARGONAUTE1* (*AGO1*) gene likewise fail to develop axillary meristems (Talbert et al., 1995; Bohmert et al., 1997). Unlike *pnh* mutants however, *ago1* and *revoluta* mutants exhibit leaf abnormalities. *revoluta* leaves are longer and narrower than wild-type leaves while *ago1* leaves are narrow with a thickened blade and sometimes are radially symmetric.

The *AGO1* and *PNH* genes encode related proteins of unknown function (Bohmert et al., 1997; Moussian et al., 1998). Moussian et al. (1998) recently have described the molecular identification of the *PNH* locus. Here we provide independent confirmation and extend molecular characterization of the *PNH* gene and its expression pattern. We expand our description of the effects of *pnh* mutations on development. Based on these results we propose that *PNH* is a candidate for a factor that confers competence to form SAMs. Additionally, we describe the expression pattern of the *AGO1* gene and the phenotype of individuals homozygous for mutations in both *PNH* and *AGO1*. These studies indicate that *PNH* plays a role in early stages of embryogenesis and overlaps in function with *AGO1*.

MATERIALS AND METHODS

Growth conditions

Plants were grown at 24°C under continuous cool white fluorescent light in Metromix 200 (Grace, Sierra) unless otherwise noted. Sterile medium was MS (Sigma, St. Louis, MO) with 2% sucrose. Where indicated, kanamycin was added to a concentration of 50 µg/ml.

Gibberellin (10 µM GA3) was added to promote germination of *ago1* mutant seedlings, which were then transferred to standard medium.

Genetics

The *pnh-8* allele arose spontaneously in a line segregating *cup-shaped cotyledon2* (*cuc2*). Other *pnh* alleles were induced by EMS. *pnh-11* was a gift from Yuval Eshed and John Bowman. *pnh-9* was a gift from Alan Jones and Scott Poethig. Mutant lines were backcrossed at least twice to Landsberg *erecta* (Ler) and determined to be linked to *TT3* on chromosome V.

Allelism between *pnh-8* and *pnh-2* was established by crossing a *pnh-8* homozygote to a *pnh-2* homozygote; 30/30 progeny displayed a short carpel phenotype indicating non-complementation. Similar results were found for *pnh-8* and *pnh-4*.

Wild-type revertants were isolated by screening homozygous *pnh-8* plants for reversion of the short carpel phenotype to wild type.

The *ago1-7* allele arose in a Ti-DNA mutagenized population (Höfte collection; Wassilewskija ecotype) while the *ago1-8* allele arose following EMS mutagenesis (Ler ecotype). The *ago1-7* allele is assumed to be allelic to the published *ago1* alleles because a Ti-DNA is inserted at codon 571 of the *AGO1* coding sequence. The *ago1-8* allele fails to complement *ago1-7*; 12/53 progeny from the cross *ago1-7/+* by *ago1-8/+* exhibited the *ago1* phenotype. The *ago1-7* line, which contains a single Ti-DNA insertion (data not shown), was outcrossed to Ler once before crossing to *pnh-2* for double mutant analysis. *ago1-8* was backcrossed twice to Ler before crossing to *pnh-2*.

Homozygous *pnh-2* pollen was crossed onto heterozygous *ago1-7* plants. The resulting *ago1-7/+*; *pnh-2/+* F₁ plants produced both *ago1* and *pnh* mutants in their self-progeny. Six phenotypically *pnh* plants were chosen from the self-progeny of an *ago1-7/+*; *pnh-2/+* parent. Of these, three were heterozygous for kanamycin resistance and three were homozygous for kanamycin sensitivity as determined by progeny testing. Neither class gave rise to *ago1* mutants in their self progeny. However, the heterozygous kanamycin resistant plants produced 25% shriveled seeds ($n=172$). We conclude shriveled seeds are homozygous for both *pnh* and *ago1* mutations.

Histology

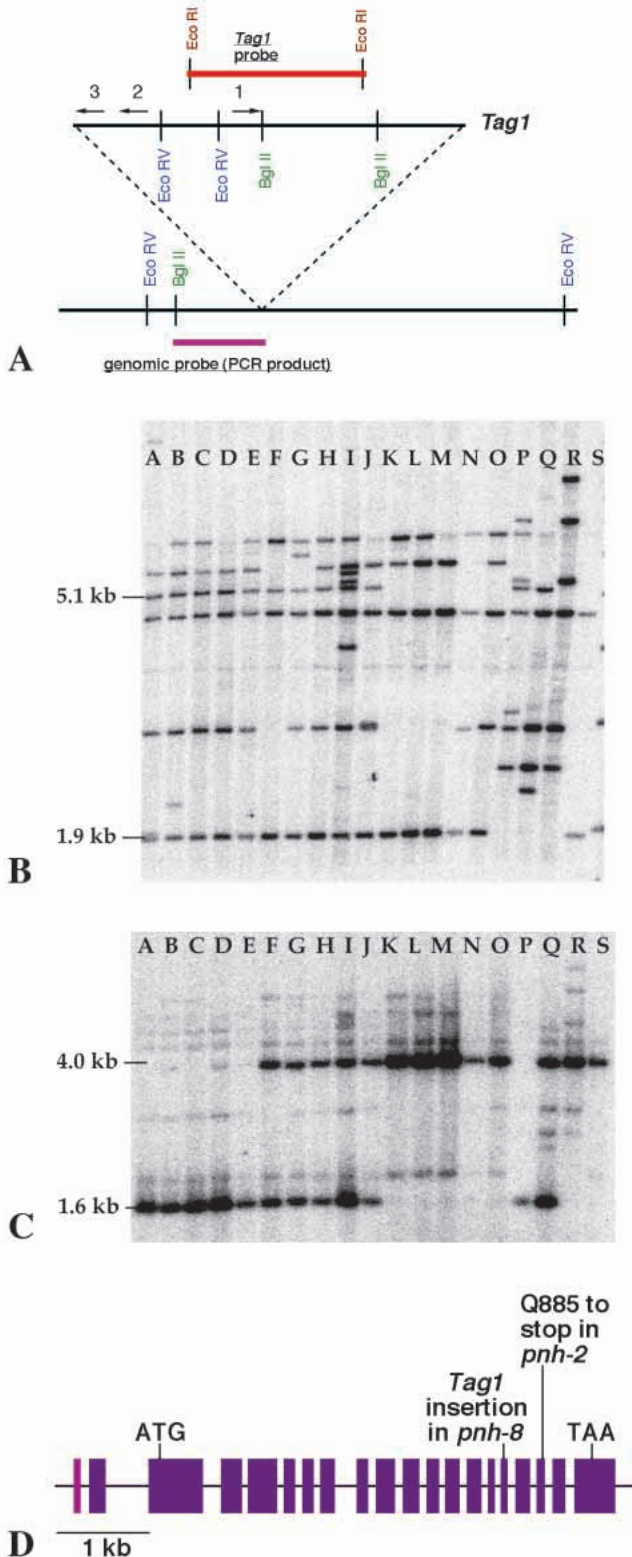
For scanning electron microscopy, specimens were processed as described by McConnell and Barton (1995). For light microscopy,

Fig. 1. (A) Restriction map of *Tag1* insertion in *pnh-8*. Arrows indicate IPCR primers. The large triangle represents *Tag1*. Red lines above and below map indicate Southern blot probes. (B,C) Southern blots showing association between presence of a *Tag1* element and the *pnh-8* mutation. Genomic DNA was digested with *EcoRV*, Southern blotted and probed with the *Tag1* probe (B) or flanking genomic probe (C). Lanes A-O: individual F₂ segregants from a cross of *pnh-8/pnh-8* by Ler. Lanes A-E: *pnh-8/pnh-8*; lanes F-J: *pnh-8/+*; and lanes K-O: *+/+*. The 5.1 kb *EcoRV* band in B and the 1.6 kb *EcoRV* band in C cosegregate with the *pnh-8* mutation. Lanes P (*pnh-8/pnh-8*), Q (*pnh-8/pnh-8r*) and R (*pnh-8r-pnh-8r*): self-progeny of a revertant from a homozygous *pnh-8* line. The 5.1 kb band (B) and the 1.6 kb band (C) are missing in the homozygous revertant. Lane S: Ler. The 1.9 kb band in B was absent from the original *pnh-8* line and is not found in the revertants. (D) Map of genomic *PNH* region showing introns (lines), exons (boxes), and predicted translation start site. Lighter box at 5' end represents the alternative first exon of the 5' UTR reported in Moussian et al. (1998). (E) Alignment of Ler *PNH*, rabbit *eIF2C* and *AGO1* amino acid sequences. Region corresponding to the *PNH* probe (pKL3) and the *AGO1* probe (pKL11) used for in situ and northern blot experiments is indicated by a red line above the sequence. The region within the blue box differs from the published *ZWILLE* sequence.

specimens were processed as described by Barton and Poethig (1993). For in situ hybridizations and immunolocalizations, specimens were processed as described by Long et al. (1996).

The rat anti-STM antibody was raised against a 15 kDa peptide outside the homeodomain. 402 bp of the *STM* cDNA (residues 126-255) was amplified using primers flanked by *Nde*I and *Bam*HI

restriction sites. The PCR product was cloned into expression vector Pet15b (Novagen, Madison, WI). Expression was induced in *E. coli* host cells B121 (DE3) pLysS, and the overexpressed protein was purified by isolation of inclusion bodies and subsequent gel purification of the 15 kDa peptide. Four rats were injected with the 15 kDa peptide at the University of Wisconsin Animal Care Facility.



PNH
eIF2C
AG01

MPHQMDSS---EPLHLVKTQTLK-----HNPKTVQNK-
LVRKRRITAPSEGGEGSGSREAGIVSGGGGRSGRGGFQQGGGQFGGGRGY
TFPSPSPVTVTTPATVTSASSPSP---SKNRSSRRNRNGGRKS-DCG
TFCQGGGRGGRGYQGPFCQQQYGGQEQYQGRGEGGPPHOGRRGGYGGC
DVCMRPSPSRKPPF-----SCVTSASVAVATAGTIVAVN
RGGGFPSSGIFQRQSVBELHQATSPTYQAVSSCFILSEVPTQVIEPTVLA
HQMCMGV-----FKNSTFAHRPGFTLTKCIVKANHF
CQFCLSGVEQGAPSQAIQPIPPSSSAFKFPMRPGKQSEKPCIVKANHF
ADLTKPLNOYDVITTFEVSSEKSNMRAIALVRLHYKESDLGRRLPAYDG
LIFKILHYHVELLTPKPCFRVNRNIEVHHVQHLKAOIFEDRKFVDD
BELLDKDLHYDVTITFEVTSRGVNRNAVMLKDLNDRNHLGSRLPAYDG
RKSLYTAGELPTWKEFSVKIVDEDDIINQPKRERSYKVAIKFVARENM
RNLVITAMPLHIGREKVELEV-----TLFGCEKIDRFKVSILKMSVCSVL
RKSLYTAGLPLSKWKEFRINLLDEVEAAGQRRREBFKVVTKLVARADL
HHLCFFIAGKRAICFOEAVQILDVIRELSVHRCFVGRSFFSPDIKTFG
QALHDAFSCRLPSVEETIQALDVWRHLPSMYTPVGRSFTASECCSN
HHLCMFLEGKQSDAFQELQVLDVIRELFTSRVTPVGRSFTSPDIEKKQ
RLGGLESVCGFYQSIRPTQMGLSLNIDMSAAPTLEPLVIEFVAQLIG
PLGGREFVWGFHOSVRSPLWMMNLNIDVSAFAYKQVPIEFVGEVDDF
SLGGLESVCGFYQSIRPTQMGLSLNIDMSSTAFIEANVIEFVCDLLN-
KDIVL---KPLSDSDSRVHKIKKLRGVKVEVTHRGVNRKRYVAGLTCTPR
KSLDEQKPLIDSRVHFKEIKLWELITGCMRKKRYCNVNRRAES
RDLSS---RPLSIDRVKIKKLRGVKVEVTHRGVNRKRYKISGLAVATR
EIMFPVDENCTM---SVIEYHQBMYGHTIQHHTLPCLOVGRQKASVLP
HCTFFLQSGSGTVECTVAGYHKDRHKLVLRYHILPCLOVGRQKHTLYL
ELTFPEVDERNIQ---SVVEYHQBMYGHTIQHHTLPCLOVGRSNRPNLYL
MEACKIVEGORYAKRLNEHQITALKLVTCORFDRENDILITVQHNADQ
IEVCNIVAGORCKIKITDNCSTMTIRTAARSADREBEHSLKLMRSASNT
MEVCKIVEGORYSKRLNDRQITALKLVTCORFDRENDILITVQHNADQ
DPYAEKFGMNIESTASVEARILLAPWLKYHENGKERDCLPOV-GQWMN
DPYVEFEGIMVKMDITVGRVLCPSILY---GGKKAIAATEVQVMDMR
ENVAECFGIKISTASVEARILLPPWLKYHESCREGTCLPOV-GQWMN
NKKMINGMTVNRWA---CVNPSRVOENVARCFNEGCOMCEVSGMFPNPE
NKHPTLEIKVNAIACPAQCTVEHLSKEFQRKISRDAAGPIQGO
NKKMINGTVMNMI---CINPSROVQDLARTFCQELQMCVYSGMAFNPE
PVILIYSARPDOVERALKHVYHTSMNN-TKKELELILALPDDNNGSLYC
FCFCYVQAQAGSVPGMFRLKNTYAG-----IQVVVILBGT-PVVA
ILVLPVPSAREQEVKLRTRYHDAISLSQSKEDILILVLPDDNNGSLYC
DLKRICTELGLISQCLTKHVFYSKQYLADEVSLKINVKVGGRRNTVLVD
EVKRVGIVLGMAIQVOMRQWORTHCTISNCLKINVKLGCVNHI-
DLKRICTELGLISQCLTKHVFYSKQYMANVALKINVKVGGRRNTVLVD
RISCPRLVSDIPTIFPGADVTHEGEBDESSPSIAAVVASQDWPEVTKYA
ILPGREFVQGVITFLPGADVTHPGDGKPSIAAVVASMD-AHPNFKY
ALSRRILVSDRPTIFPGADVTHEGEBDESSPSIAAVVASQDWPEVTKYA
GLVCAQAHRQELIODEYKWDQFVRCVSGGMRELLIESRSTCKPLR
ATVRVQGHREITODI-----AAMRELLIESRSTCKPLR
GLVCAQAHRQELIODEYKWDQFVRCVSGGMRELLIESRSTCKPLR
IIFYRDGVSEGOFYQVLLYELDAIRKACASIPNYQPPVTFIVVQKRHHIT
EIFYRDGVSEGOFYQVLIHEITAIREACIKLEKQYHGHTFIVVQKRHHIT
IIFYRDGVSEGOFYQVLLYELDAIRKACASIPNYQPPVTFIVVQKRHHIT
RLFAANNRKNKSDRSNGLPGTVDDTKICHPTEFFDFYLCSHAGIQGTSR
RLFCTDRNER-VKSGSNIPTACTVDTKICHPTEFFDFYLCSHAGIQGTSR
RLFAQNHNDRESVDRSGNILPGTVVDSKICHPTEFFDFYLCSHAGIQGTSR
PAHYHVLWDENNFTADGLQSLTNNLKCYTYARCTRSVSIVPPAYYAHLAA
PSHYHVLWDNRSSDELLITVLCQTYARCTRSVSIPAPAYYAHVAF
PAHYHVLWDENNFTADGLQSLTNNLKCYTYARCTRSVSIVPPAYYAHLAA
RARFYLEPFI-----MCDNCSGPKKNSTTVIGDVCKPLPALKE
RARVHVDKDHSAEGSH7SGSGNRDQHAAVVOHDTL-
RARFYMEPFTSDSGSMASGSMARCGMAGRSIRGPIV-NAATPLPALKE
NVKRVMFYC
---TMTFA
NVKRVMFYC

E

Raw serum from one of these rats was used for immunolocalizations as described by Perry et al. (1996).

Determining *PNH* gene structure

A *pnh-8* specific 2.3 kb *Bgl*II genomic DNA fragment was gel purified and intramolecularly ligated. Nested inverse PCR was performed using the primers indicated in Fig. 1A; sequences were: no. 1 cgtcctggagaaacacgtttt; no. 2 tcgtgggttaatagcgggtt; no. 3 ttccggtcgggcgtgaaaa.

DNA sequences were determined for both strands using Amplitaq (Perkin-Elmer, Foster City, CA). The sequence of 9.8 kb of genomic DNA from the cd4-8 library (ecotype Ler) was determined. Three overlapping cDNA clones were isolated from the cd4-16 cDNA library (ecotype Columbia). The 5' end of the cDNA was isolated by reverse transcription of poly(A)⁺ RNA from Ler plants using primer KLN-5.5 (ataccgtcatcttcaacaattcta) followed by amplification by PCR using primers KLN-5.5 and KLC-8.5 (tctccgggatctcattt). Exon-intron boundaries are based on a comparison of the cDNA and genomic sequences. No amino acid differences were observed between Ler and Columbia ecotypes.

Sequences of mutant alleles were determined by first amplifying the *pnh* gene from mutant genomic DNA with PFU polymerase (Stratagene, La Jolla, CA) and cloning it into a pGEMt vector (Promega, Madison, WI). The sequence then was determined as above. Two independent amplification, cloning and sequence determination experiments were performed for each allele. For *pnh-2*, the sequence of the entire mutant gene was determined.

For Southern blots, 10 µg of restricted genomic DNA was hybridized with the *Tag1* or genomic probe (Fig. 1A) overnight at 68°C in Church buffer (0.5 M sodium phosphate, pH 7.2 and 7% SDS). For northern blots, poly(A)⁺ RNA was isolated from roots of liquid grown plants, and leaves, inflorescences, internodes and siliques of soil grown plants using PolyATtract (Promega, Madison, WI). 3 µg of poly(A)⁺ RNA was probed with the pKL3 probe (Fig. 1E). Northern blots and plaque lifts were hybridized overnight at 42°C in 50% formamide, 5× SSC, 1% SDS, 5% dextran sulfate. Blots and lifts were washed twice at 25°C in 0.1% SDS and 2× SSC for 15 minutes and once at 65°C in 0.1% SDS and 2× SSC for 30 minutes.

RESULTS

The *pnh-8* allele contains a *Tag1* insertion

The *pnh-8* mutation arose spontaneously in a line segregating *cuc2*. The homozygous *pnh-8* line carried several copies of the endogenous *Arabidopsis* transposable element *Tag1* (Tsay et al., 1993). To check for linkage of a transposon to the *PNH* locus, *pnh-8* plants were crossed to Ler plants and the resulting F₁ progeny was allowed to self-fertilize. When DNA from the F₂ plants was probed with a fragment of *Tag1* DNA, one element was found to be present in *pnh-8* homozygotes and heterozygotes and absent in homozygous wild-type plants (Fig. 1B).

To demonstrate that the linked *Tag1* element was the cause of the *pnh-8* mutation, we isolated spontaneous wild-type revertants derived from a homozygous *pnh-8* line. Two wild-type revertant individuals were found among 3481 homozygous *pnh-8* plants. The self progeny of these two revertants segregated about 1/4 *pnh* offspring (16/65 and 17/72, respectively). Progeny homozygous for either of the two *pnh-8* revertant alleles had lost the *pnh-8* linked *Tag1* element while heterozygous and homozygous *pnh-8* siblings retained the element, thus indicating that this *Tag1* insertion is the cause of the *pnh-8* mutation. A *Tag1* element characteristic of Ler was

not present in the original *pnh-8* lines and also was absent from both revertant lines, ruling out the possibility that contamination from wild-type Ler pollen caused the revertant phenotype (Fig. 1B).

A 628 bp fragment of genomic DNA adjacent to the *Tag1* element was cloned by IPCR. This fragment detects a 1.6 kb band in *Eco*RV digested DNA from homozygous *pnh-8* individuals, a 4 kb band in DNA from homozygous wild-type plants and both bands in DNA from heterozygous plants (Fig. 1C). These results are consistent with the IPCR product flanking the *pnh-8*-linked *Tag1* element. Genomic and cDNA clones were obtained using the IPCR product as a probe and their sequences were determined. The *PNH* gene consists of 19 exons encoding a predicted 988 amino acid protein (Fig. 1D). Overlapping partial cDNA clones included 157 bp of the 5' UTR, 2964 bp of coding sequence and a 229 bp 3' UTR followed by a stretch of 18 adenosine residues.

The *PNH* gene has been cloned independently by Moussian et al. (1998). Our results differ in two respects. First, the cDNA sequence we obtained indicates a 5' UTR that differs in the sequence of the first exon. Since both sequences are found in the upstream genomic DNA, this gene may have an alternative transcriptional start site or may be subject to alternative splicing (Fig. 1D). Secondly, we predict a different amino acid sequence from residues 175 to 179, located one codon 3' of the reported *zwille-13* nonsense mutation (Fig. 1E; Moussian et al., 1998). A nucleotide insertion and deletion at either end of this region are responsible for the difference.

Both *pnh-8* and *pnh-2* mutations disrupt the most highly conserved region of the *PNH* gene (see below). The *Tag1* element in *pnh-8* mutant DNA is inserted in exon 15. The resulting protein, if stable, lacks 185 amino acids of the most conserved region of the protein. *pnh-2* is caused by a nonsense mutation in exon 17 (Fig. 1D), which terminates translation amidst the most conserved region of the protein. Thus the *pnh-8* and *pnh-2* mutations likely cause substantial reduction or loss of function.

Database searches reveal significant similarity between *PNH* and the rabbit translation initiation factor eIF2C. This factor promotes formation of the ternary complex (eIF2, GTP and met-tRNA) and stabilizes the subsequent complex with the mRNA-loaded 40S ribosomal subunit (Zou et al., 1998). The first 151 amino acids of *PNH* have no corresponding portion in eIF2C. However, the amino acid identity between *PNH* and eIF2C is 35.4% from residues 151 to 672 of *PNH*, and from residues 672 to 949 of *PNH* identity is 64.3% and similarity is about 70% (Fig. 1E).

In *Arabidopsis* there are at least four members of this gene family: *PNH*, *AGO1*, *AGO1-LIKE* and at least one member defined by ESTs 95A9T7 and ATTS3322 (Bohmert et al., 1997; Moussian et al., 1998; this work). The *PNH* and *AGO1* proteins are 65% identical overall and residues 618 to 948 of *PNH* have 86% identity and 95% similarity with *AGO1* (Fig. 1E). Highly similar predicted proteins are found in other eukaryotes including humans, *Caenorhabditis elegans*, *Drosophila*, maize, rice and the single-celled yeast *Schizosaccharomyces pombe*, but have not yet been associated with a published mutant phenotype.

pnh phenotypes

Defects in meristem formation in *pnh* mutants have been

Table 1. Effect of *pinhead* mutant alleles on embryo and ovule development

Allele	Abnormal embryos	Abnormal ovules	Shriveled seeds
<i>pnh</i> ⁺ (Ler)	0.8% (n=120)	0% (n=120)	0.4% (n=250)
<i>pnh-2</i>	6.3% (n=165)	2.0% (n=151)	0.39% (n=254)
<i>pnh-4</i>	14% (n=164)	4.9% (n=164)	1.8% (n=275)
<i>pnh-8</i>	12% (n=33)	9.1% (n=33)	1.8% (n=225)

described previously (McConnell and Barton, 1995; Moussian et al., 1998). We have identified additional phenotypes associated with *pnh* mutations. In particular, abnormal embryos are found at a higher frequency in siliques of homozygous *pnh* plants than in the wild-type (Table 1). These embryos display defects in development of the basal portion of the embryo proper or of suspensor-derived cells (Fig. 2A). These early defects apparently do not lead to developmental arrest, since defective embryos are not obvious at later stages of embryogenesis (e.g. heart stage and beyond; data not shown) and fewer shriveled seeds are found than abnormal early embryos (Table 1).

None of the *pnh* mutant alleles isolated to date are completely penetrant with respect to the effects on embryonic SAM formation (Table 2). A proportion of *pnh* homozygotes, ranging from 26% to 90%, forms apparently normal SAMs. This is true even for the presumed loss-of-function alleles *pnh-2* and *pnh-8*. When a SAM is not properly formed, it may terminate in (in decreasing order of severity) a flat meristem, a small radially symmetric pin-like structure that lacks a vascular strand, a radially symmetric leaf, a single leaf or two leaves fused on their adaxial sides (McConnell and Barton, 1995; Fig. 2B,C; Table 2).

Axillary meristems often are absent in *pnh* plants (McConnell and Barton, 1995; Fig. 2D). This defect is associated with all mutant alleles and is observed more frequently in the axils of primary inflorescences than in the axils of secondary inflorescences (Table 3; this difference is significant at $P < 0.01$ for all alleles). As for the primary SAM defect, the axillary SAM may either be missing or replaced by a terminally differentiated organ such as a leaf or filament.

Table 2. Effect of *pinhead* mutant alleles on the development of the primary shoot apical meristem

Allele	Normal meristem	Fused leaves	Single leaf	Pin	Flat meristem
<i>pnh</i> ⁺ (Ler, n=500)	100%	0%	0%	0%	0%
<i>pnh-2</i> (n=171)	51%	2%	7%	27%	13%
<i>pnh-4</i> (n=110)	90%	0%	5%	5%	0%
<i>pnh-8</i> (n=154)	56%	2%	11%	21%	10%
<i>pnh-9</i> (n=46)	26%	0%	24%	22%	28%
<i>pnh-11</i> (n=127)	80%	1%	6%	7%	6%

Although fasciation is observed in *pnh* mutants, albeit infrequently, we conclude that the axillary meristem defect is not secondary to fasciation since axils that lack buds are found on non-fasciated stems. Furthermore, in *clavata1* and *clavata3* mutants, both of which often exhibit fasciation, buds are present in all axils examined ($n=100$ axils for *clavata1-4* and for *clavata3-2*).

The most penetrant phenotype of *pnh* mutants is found in the flower, where the silique is composed of two to four carpels and always is at least 50% shorter than in the wild type (Fig. 2E,F; Table 4). 100% of *pnh* homozygotes show a short carpel defect indicating that carpel development is especially sensitive

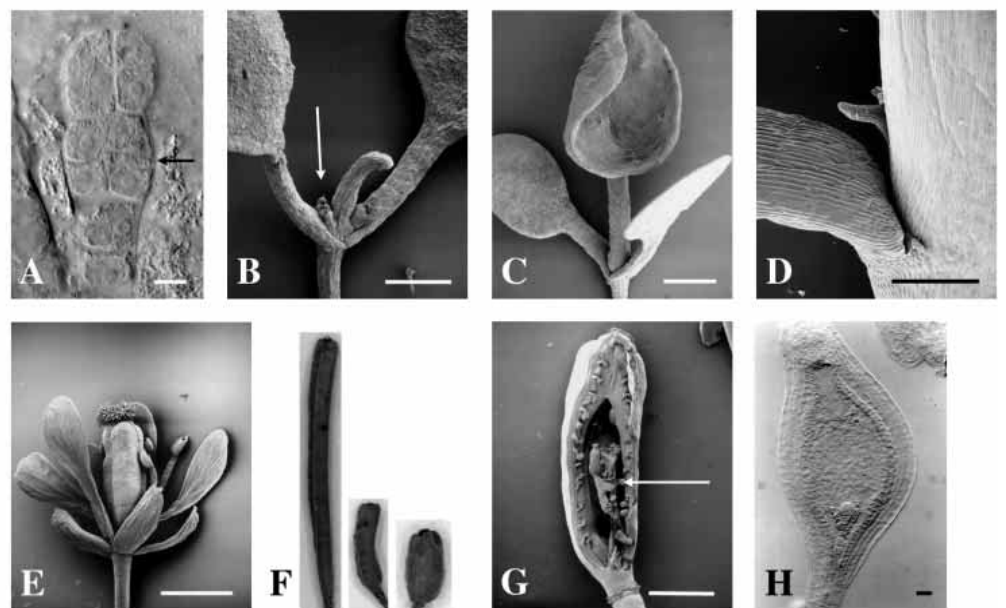


Fig. 2. Phenotypes associated with *pnh* mutants. (A) Abnormal embryo. The upper cells of the suspensor have divided aberrantly (arrow); see Fig. 3B for wild-type appearance. (B) Seedling in which a radially symmetric pin-like structure is in the position normally occupied by the SAM. After a delay, new meristems arise in the axils of the cotyledons (arrow). (C) Seedling in which a trumpet-shaped leaf is in the position normally occupied by the SAM. Adaxial tissue is on the inside of the 'bell', abaxial on the outside. (D) Primary inflorescence axil showing barren axil phenotype. (E) Flower in which the gynoecium is made up of several carpels. (F) Siliques from wild-type Ler (left), *pnh* (center), and *ago*^{+/+}; *pnh/pnh* plants. (G) Arrow points to ectopic carpels found interior to the normal fourth whorl carpels. (H) 'Linear' ovule. Bar, 25 μ m (A,H); 1 mm (B,C,E,G); and 250 μ m (D).

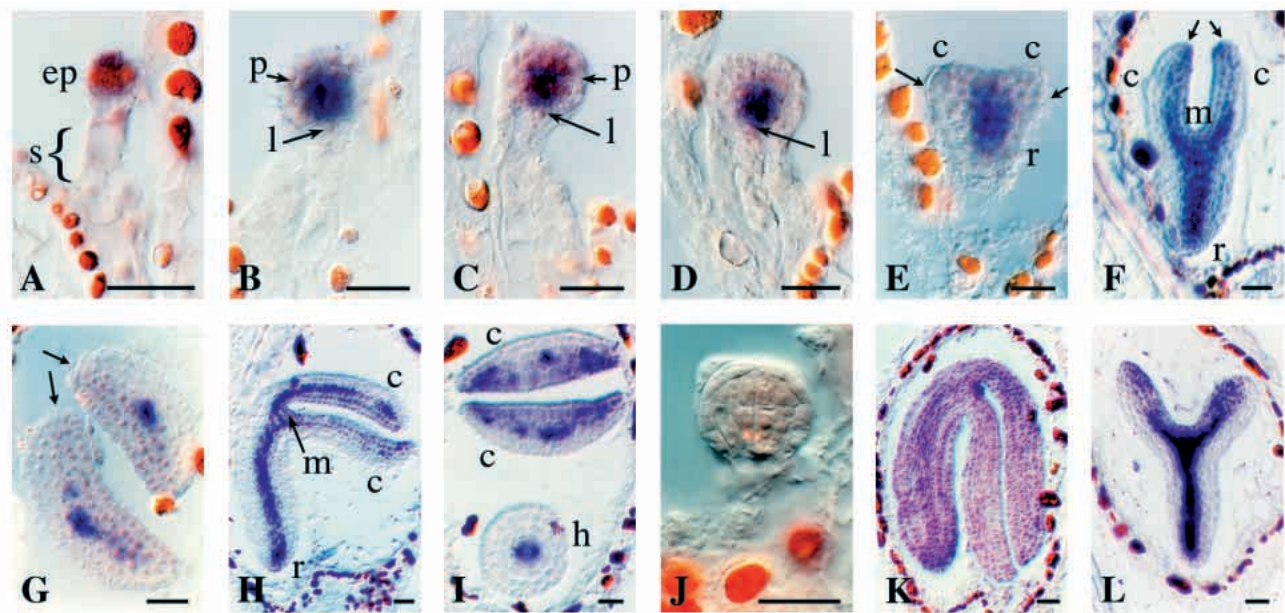


Fig. 3. *PNH* mRNA accumulation during embryogenesis. Unless indicated otherwise, embryos were hybridized to an antisense *PNH* probe (pKL3; Fig. 1E). A–K are wild-type embryos. L is *ago1-7/ago1-7*. (A) Four-cell stage. (B) Dermatogen stage. (C) Globular stage. (D) Early transition stage. (E) Late transition-early heart stage. (F) Torpedo stage. (G) Transverse section through cotyledons at torpedo stage. (H) Walking stick stage. (I) Transverse section through a nearly mature embryo. (J) Globular stage embryo hybridized to a sense *PNH* probe. (K) Fully developed embryo hybridized to an antisense probe for *UBIQUITIN4*. (L) Torpedo stage *ago1* embryo. c, cotyledon primordium; ep, embryo proper; h, hypocotyl; l, lenticular cell; m, presumptive SAM; p, protoderm layer; r, root pole; s, suspensor. Arrows indicate adaxial/abaxial boundary. Bar, 25 μm.

to mutations in *PNH*. Additional carpels occasionally develop interior to the fourth whorl carpels (Fig. 2G).

Table 3. Axillary meristem formation in *pinhead* mutants

Allele	Primary inflorescence	Secondary inflorescence
<i>pnh</i> ⁺ (Ler)	100% normal 0% barren 0% leaf or filament (n=57)	100% normal 0% barren 0% leaf or filament (n=109)
<i>pnh-2</i>	83% normal 15% barren 1% leaf or filament (n=78)	56% normal 42% barren 2% leaf or filament (n=43)
<i>pnh-4</i>	88% normal 12% barren 0% leaf or filament (n=57)	47% normal 49% barren 4% leaf or filament (n=79)
<i>pnh-8</i>	94% normal 4% barren 2% flower (n=67)	47% normal 51% barren 2% leaf or filament (n=45)
<i>pnh-9</i>	80% normal 17% barren 3% leaf or filament (n=94)	53% normal 44% barren 2% flower (n=45)
<i>pnh-11</i>	100% normal 0% barren 0% leaf or filament (n=62)	41% normal 56% barren 2% leaf or filament (n=41)
<i>pnh-2; ago/+</i>	80% normal 14% barren 4% leaf or filament (n=77)	45% normal 50% barren 5% leaf or filament (n=44)

The numbers of other floral organs are affected as well with both more and fewer organs observed (Table 4). In some cases, the average number of floral organs was the same as in wild type, but the range and standard deviations were greater (e.g. the number of sepals in *pnh-4*).

Wild-type *Arabidopsis* ovules grow differentially on their ad- and abaxial sides so that the micropylar end lies adjacent to the funiculus. In *pnh* mutants, some orthotropous, or straight, ovules were observed in mutants for all alleles examined (Fig. 2H; Table 1).

Roots from seedlings homozygous for *pnh-2* and *pnh-8* were examined for their rate of growth, for their ability to form lateral root meristems and root hairs and for cellular organization along the radial axis. No differences were observed relative to wild type (data not shown).

Thus, we conclude that *pnh* mutations are highly pleiotropic, affecting embryo development, primary and axillary SAM formation, floral organ number and shape and ovule morphology. Interestingly, it has not been possible to construct an allelic series based on all the phenotypes reported above as each allele seems to affect these processes differentially.

***PNH* mRNA expression**

PNH mRNA accumulation was examined on a northern blot using the pKL3 probe, which detects a single 3.6 kb transcript in roots, stems, leaves, siliques and inflorescences (data not shown). Expression was examined further by hybridizing tissue sections to the same probe.

In the embryo, *PNH* mRNA is detected by the four-cell stage when accumulation is found in the embryo proper and there is light staining in the uppermost cell of the suspensor (Fig. 3A). As development proceeds, the message is

Fig. 4. Transverse sections through vegetative meristems showing expression of *PNH* mRNA (A,B,D-F,H,I) and STM protein (G). (A,B and D-F) Serial sections (8 μ m thick) through a single short-day grown, 17-day old, vegetative meristem. (C) Diagram based on section in B showing the location of the primordia. Yellow circles represent areas of intense *PNH* expression as compiled from all serial sections. Note that the region of high *PNH* expression in each primordium falls just outside the line connecting the region of high expression for the second and third previous primordia, demonstrating that the areas of high expression within the SAM coincide with the expected location of p0 and p-1. (G) Section similar to those in B and D from a similar seedling. (H) Enlargement of the region indicated by an arrow in D. (I) Transverse section through a wild-type leaf primordium. m, meristem; lp, leaf primordium; p1, primordium one. Numbers in top left of each panel indicate the number of microns below the apex the section represents. Arrows in B,D and H indicate differential *PNH* stain in p1; arrow in F indicates *PNH* stain in p-1. Bar, 100 μ m for A-G and 25 μ m H-I.

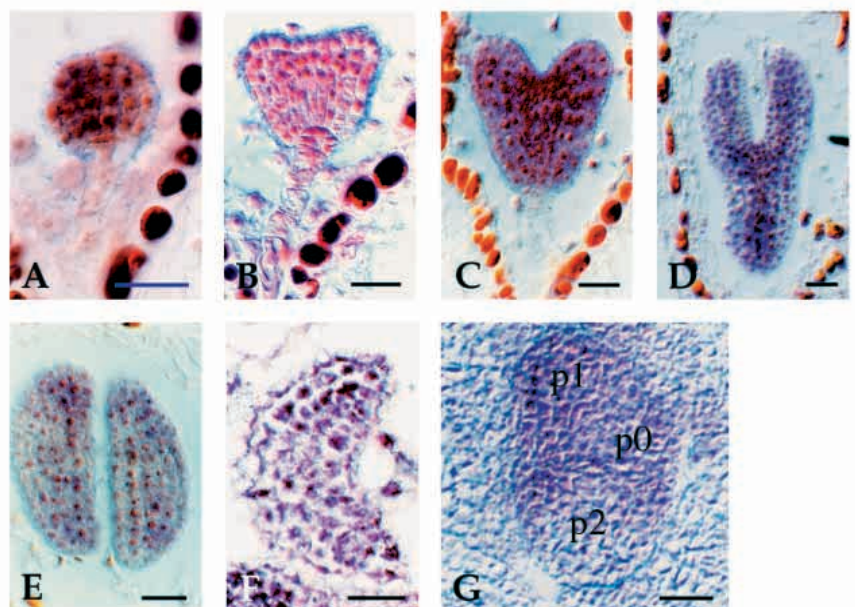
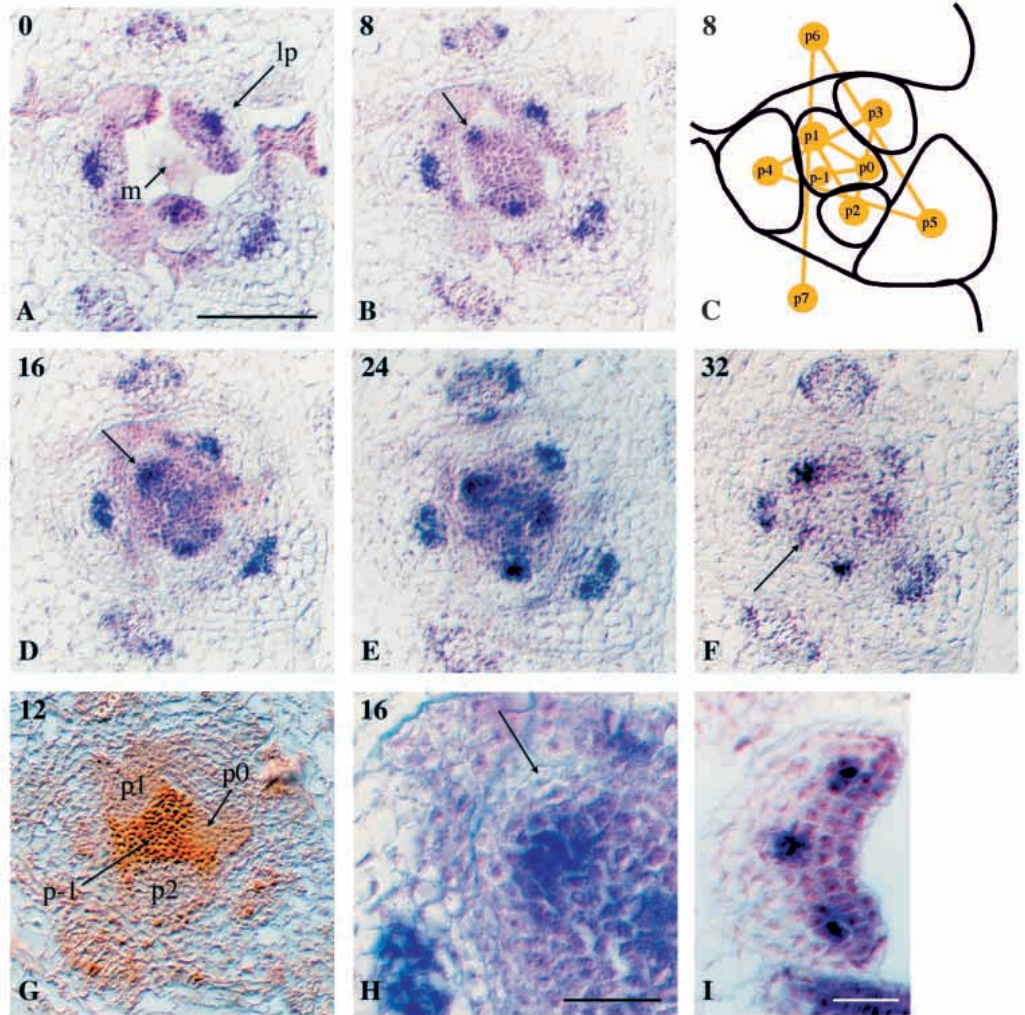


Fig. 5. *AGO1* mRNA accumulation in wild-type development. Probe is an antisense *AGO1* probe (pKL11; see Fig. 1E). (A) Globular embryo. (B) Late transition-early heart stage embryo. (C) Heart stage embryo. (D) Torpedo stage embryo. (E) Transverse section through cotyledons of torpedo stage embryo. (F) Transverse section through leaf primordium. (G) Transverse section through short day grown, 17-day old vegetative meristem; depth is about 8 μ m. p1, primordium one. Bar, 25 μ m.

progressively confined to central and adaxial areas and is expressed at two intensities. *PNH* message is evenly distributed throughout the embryo proper until the dermatogen stage, when staining appears lighter in the protoderm (Fig. 3B). At the globular stage, the provascular cells stain intensely, while the protoderm and lenticular cell stain lightly and no stain is detected in the lower protoderm (Fig. 3C,D). By early heart stage, the lighter stain spans the cells expected to give rise to the adaxial sides of the cotyledons and the SAM, and is in the derivatives of the lenticular cell in the root pole (Fig. 3E). The boundary between lightly staining and non-staining cells bisects the cotyledon primordia along their ad/abaxial axis (Fig. 3E-G, arrows).

At torpedo stage, the dark stain in the provascular cells expands up the center of the cotyledons. Light staining appears only adaxial to this stripe of expression in the cotyledons and is still in the SAM and root pole (Fig. 3F). A transverse section through the cotyledon primordia at this stage demonstrates differential expression between their ad- and abaxial sides (Fig. 3G). This pattern is stably maintained through the walking stick stage (Fig. 3H). Transverse sections through a nearly mature embryo reveal dark staining in the procambium of the root-hypocotyl axis, lighter staining in the primary xylem precursor area and a pattern of dark staining in the cotyledons that corresponds to the pattern of vascular strands in the mature cotyledon (Fig. 3I). Thus *PNH* mRNA is detectable at two levels in the embryo: intense staining marks the vascular precursors and light staining marks the adaxial sides of the cotyledons and the two apical meristems.

After germination, *PNH* expression persists in the vegetative meristem. Similar to the embryonic pattern, high-level expression is detected in developing vascular strands while low-level expression is detected in the SAM and adaxial leaf domains. Fig. 4 shows serial sections through the apex of a short-day grown plant. Two leaf primordia, p0 and p1, are detectable in the vegetative SAM as areas that are not marked by the *STM* antibody (Fig. 4G). *STM* is expressed throughout the SAM except at positions of developing leaf primordia. P0 is contained entirely within the SAM, and p1,

while often difficult to distinguish as separate from the SAM, has begun to grow outward. While p0 expresses *PNH* uniformly (Fig. 4E,F), p1 exhibits some differential expression of *PNH* along the ad/abaxial dimension (Fig. 4B,D,H) indicating that by the p1 stage the primordium has acquired polarity in the radial dimension. By the p2 stage, outgrowth from the SAM is conspicuous and differential *PNH* expression is more distinct.

Each leaf primordium develops in association with a high-density region of *PNH* expression that marks the presumptive leaf trace, the vascular strand that extends from the stem to the leaf. This high-intensity stain extends further apically in older primordia than in young leaf primordia. To illustrate, high-intensity *PNH* expression associated with p1 is detectable 8 µm below the apex of the SAM, while expression associated with p0 and p-1 is found at 24 µm and 32 µm, respectively (Fig. 4). Note that *STM* down-regulation is not observed in p-1 making the leaf trace-associated *PNH* expression an earlier marker of leaf formation.

The specificity of the pKL3 probe on the northern blot indicates that the pattern seen in situ is attributable to expression of the *PNH* gene alone. To confirm further that the pKL3 probe did not hybridize to a related sequence, we performed a separate set of experiments using a probe corresponding to the 5' UTR and the first 472 bases of coding sequence. This probe gave the same pattern of expression as that seen with pKL3 (data not shown). We also used a probe to the *AGO1* gene (pKL11, Fig. 1E) to determine if we would see a different pattern of hybridization with this closely related family member. Although the *AGO1* sequence is 70% identical to the *PNH* gene in this region, the differences in the expression patterns of *AGO1* (described below) and *PNH* confirm that the *PNH* probe does not detect *AGO1* mRNA in our experiments.

The *AGO1* transcript is expressed as early as the globular stage (Fig. 5A). While *PNH* mRNA accumulation is detectable at two levels, *AGO1* message is evenly distributed throughout the embryo proper and is present in the suspensor (Fig. 5B). This pattern continues throughout embryogenesis (Fig. 5B-D). A cross-section through the cotyledons of a torpedo stage embryo demonstrates that, unlike *PNH* mRNA, *AGO1* mRNA does not accumulate differentially in the adaxial regions of the cotyledons (Fig. 5E). Likewise, in seedlings the *AGO1* transcript is evenly distributed throughout the SAM and leaf primordia (Fig. 5F,G).

ago1 phenotype

The finding that *PNH* and *AGO1* encode related proteins and are expressed in overlapping domains prompted us to ask whether these genes play redundant roles. Mutants homozygous for the *ago1-7* and *ago1-8* alleles, similarly to previously described *ago1* mutants, exhibit narrow, thickened rosette leaves and radialized cauline leaves that lack axillary meristems (Fig. 6B,C; Bohmert et al., 1997). In plants homozygous for mutations in *ago1-7* and *ago1-8*, the primary SAM occasionally is replaced by a single determinate pin-like organ (Fig. 6A). Thus axillary meristem and SAM defects are common to *ago1* and *pnh*, although *ago1* mutants have additional phenotypes not found in *pnh* mutants, such as radialized leaves.

The radialized leaf phenotype suggests that *ago1* mutants, like other mutants with radialized leaves such as *phb-1d*, suffer

Table 4. Floral organ number in *pinhead* mutants*

Allele	Sepals	Petals	Filaments	Stamens	Carpels
<i>pnh</i> ⁺ (Ler)	mean 4.0 range 4-4 s.d. 0	4.0 4-4 0	0	6.0 6-6 0	2.0 2-2 0
<i>pnh-2</i>	4.12 4-5 0.33	4.32 4-5 0.48	0	6.24 4-8 0.83	2.72 2-4 0.89
<i>pnh-4</i>	4.0 3-5 0.29	4.24 4-5 0.44	0.08 0-1	6.6 5-9 1.12	2.28 2-3 0.46
<i>pnh-8</i>	3.96 3-4 0.20	4.32 4-6 0.56	0.12 0-2	6.04 4-8 0.93	2.24 2-4 0.52
<i>pnh-2; ago</i> ⁺	4.10 4-5 0.3	1.95 0-4 nd	3.0 1-6 nd	6.52 5-7 0.6	3.81 3-5 0.6

*25 flowers were scored for each genotype.
nd, not determined.

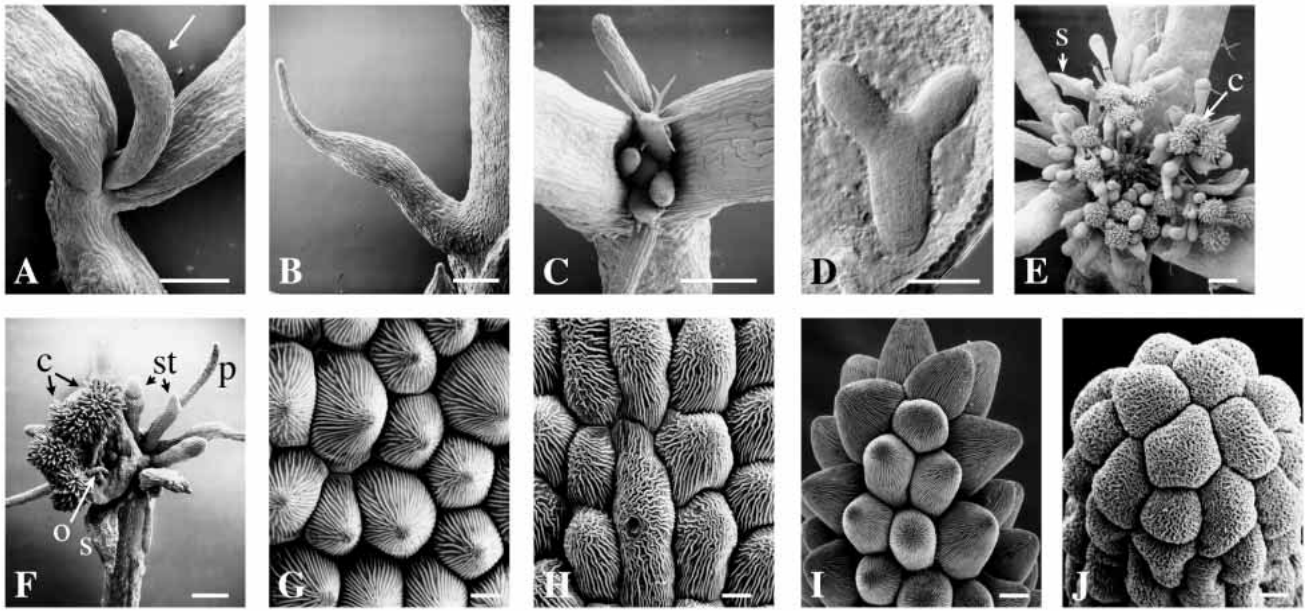


Fig. 6. Phenotypes associated with *ago1* mutants. (A) Seedling in which a terminal, *ago1* leaf-like organ has replaced the SAM (arrow). (B) Radialized cauline leaf lacking axillary bud. (C) Top view of seedling. First two rosette leaves are radial. Younger leaf primordia show more ad/abaxial flattening. (D) Torpedo stage embryo; see Fig. 3F for wild-type appearance. (E) Inflorescence. (F) Flower. (G) Wild-type adaxial petal epidermis. (H) Wild-type abaxial petal epidermis. (I) Radially symmetric, adaxialized *phabulosa* petal. (J) Radially symmetric abaxialized *ago1* petal. c, carpel; o, ovule; p, petal; st, stamen; s, sepal. Bar, 250 μ m (A-C, E, F) and 100 μ m for (D, G-J).

an alteration in organ polarity. To explore this possibility, *ago1* mutants were analyzed for polar characteristics. *ago1* sepals show flattening in the ad/abaxial dimension indicating some degree of polar development (Fig. 6E, F). However, petals are radially symmetric with abaxial epidermal cell types on the adaxial surface (compare Fig. 6G-J). Stamens are radially symmetric with a small knob at the tip (Fig. 6F). Two types of carpels are observed. One type is radially symmetric and lacks ovules (Fig. 6E); the other is unfused with ovules (Fig. 6F).

The internal anatomy of *ago1* mutant rosette leaves has normal ad/abaxial polarity (Fig. 8F) indicating that *AGO1* is not required for the development of internal leaf polarity. *ago1* leaf epidermal cells exhibit unusual morphology and cannot be characterized as adaxial or abaxial (data not shown).

During embryogenesis, we find that *ago1* mutants can be distinguished from their wild-type siblings at the torpedo stage (Fig. 6D). In wild-type embryos, initial cotyledon growth is directed outward at a roughly 45 degree angle from the long axis of the embryo; at later stages, the abaxial sides of the cotyledons grow more than the adaxial sides, resulting in close alignment of the cotyledons with the longitudinal axis of the embryo. The cotyledons of *ago1* mutants fail to make the transition from outward-directed to upward-directed growth and thus stand at a 45° angle from the embryo axis rather than vertically. This is similar to the phenotype of *phb-1d* mutant embryos in which it is thought that both sides of the cotyledons have adopted adaxial fate; such a transformation would result in similar growth rates on both sides of the cotyledon (McConnell and Barton, 1998). However, if organ polarity is affected in *ago1* cotyledons, it is not a complete transformation since *pnh* expression is found in the adaxial cotyledon domain just as in wild-type embryos (Fig. 3L).

Our characterization of polarity defects in *ago1* mutants

shows that, although some transformation from ad- to abaxial cell types occurs, not every aspect of polarity is affected. This is in contrast to the *phb-1d* mutant, in which some degree of transformation to adaxial cell types is seen in all organs. We conclude that *AGO1* is required for adaxial cell fate only in certain tissues, such as petal epidermis, or that a redundant factor is able to provide *AGO1* activity in some cell types.

ago1 pnh double mutant phenotype

Embryos mutant for both *ago1* and *pnh* fail to progress to bilateral symmetry and show retarded growth relative to wild type (Fig. 7A, B). Cells in double mutant suspensors divide inappropriately, resulting in multiple layers. To assess whether growth is completely arrested, we counted cells in double mutant embryos at two stages. Mutant embryos whose siblings were at the torpedo stage consisted of about 100 cells. Mutant embryos whose siblings were mature consisted of about 160 cells indicating that growth continues, although at a very slow rate, in the mutant.

Since both *ago1* and *pnh* mutants exhibit defects in meristem formation, we analyzed STM protein expression in single and double mutant embryos. Normally, STM is detectable in the presumptive SAM by the late globular stage (A. Fernandez, unpublished results) and persists in the meristem throughout embryogenesis. While both single mutant embryos express STM during embryogenesis, double mutant embryos did not detectably accumulate STM protein (Fig. 7C-F). Double mutant embryos of all stages were examined, and STM accumulation was not detected at any point during embryogenesis, although postembryonic expression cannot be ruled out.

Although shriveled, seeds carrying the double mutant embryos are desiccation tolerant and germinate, albeit with a

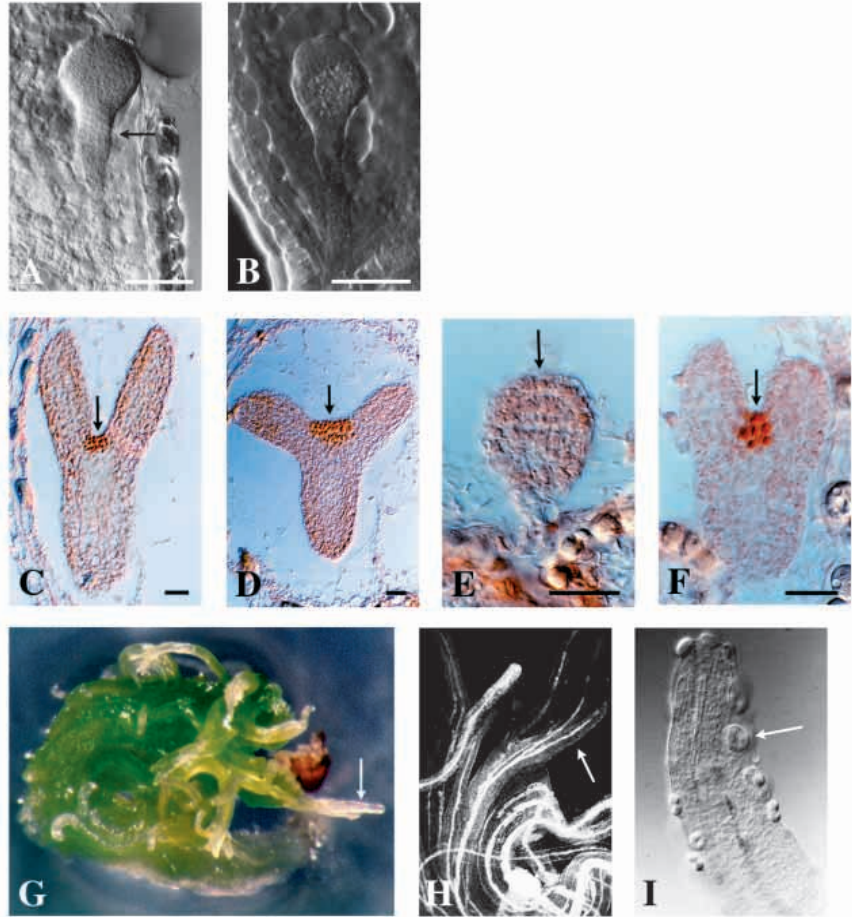


Fig. 7. Phenotype of *ago1 pnh* double mutants. (A) Abnormal mutant embryo. Siblings in the same silique were at torpedo stage. Note extra divisions in the upper cells of the suspensor (arrow). (B) Abnormal mutant embryo at maturity. Siblings in the same silique were fully developed embryos. (C-F) STM protein localization. All embryos are from the self-progeny of an *ago*^{+/+}; *pnh*^{+/+} parent. Arrow in each panel indicates position where presumptive SAM is expected. (C) Wild-type appearing embryo at late torpedo stage. (D) *ago1* embryo. Wild-type siblings were at walking stick stage. (E) Presumed double mutant embryo. (F) Sibling embryo from the same silique as embryo in E. (G) Seven-week old double mutant. Arrow points to filamentous outgrowth. (H) Plant in G, cleared and viewed with dark-field optics. Arrow points to filamentous structure. (I) Close-up of filament. Arrow points to stomate. Bar, 25 μ m.

several week delay. The resulting seedlings are highly abnormal (Fig. 7G). The shoot system is disorganized, producing slender, filamentous organs in an unpredictable arrangement. These organs have stomata on their epidermis and contain xylem elements (Fig. 7H,I). However, xylem elements are not always arranged in a contiguous strand and individual xylem cells often are misshapen. Double mutant individuals show evidence of a root/shoot axis (clear cells at the base of the seedling, green cells toward the apex) and of the three types of cell layers (vascular, ground, and epidermal tissue).

Thus, the *PNH* and *AGO1* genes act redundantly to allow wild-type growth rates and wild-type patterns of gene expression during embryogenesis. These genes are not strictly required for viability nor are they required for the development of the embryo axis or three basic tissue layers.

***ago1* and *pnh* mutations behave dominantly in *pnh* and *ago1* homozygous mutants, respectively**

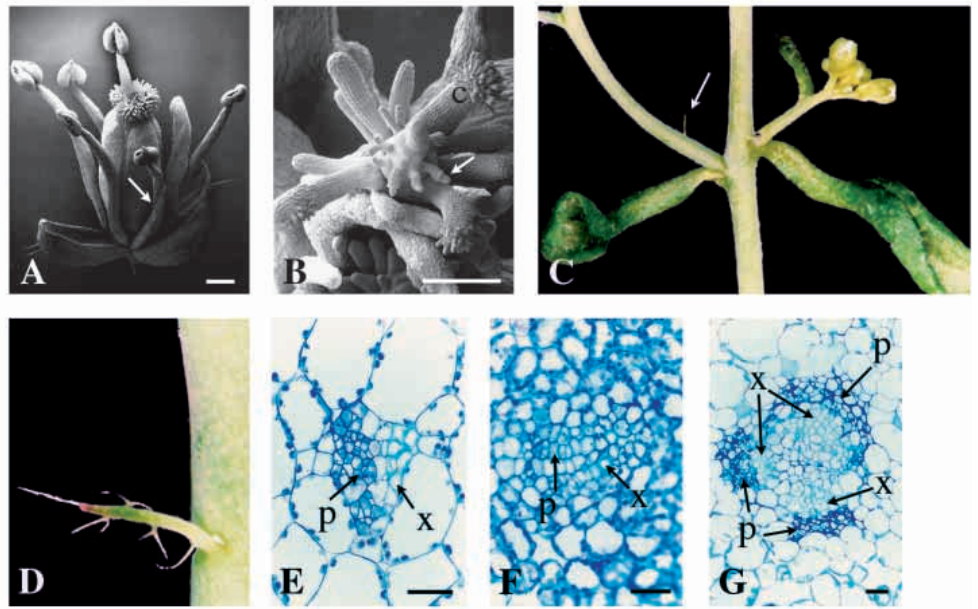
AGO1 and *PNH* encode partially redundant, homologous genes that are required for normal embryogenesis. If they also act redundantly during postembryonic development, we might expect that lowering the dose of one gene in the homozygous mutant background of the other would yield a novel, dominant phenotype. Indeed, both *ago1* and *pnh* mutations are incompletely dominant in plants homozygous for *pnh* and *ago1*, respectively.

Offspring of kanamycin resistant homozygous *pnh-2* plants were chosen for study. (Kanamycin resistance is linked to the *ago1-7* mutation.) *ago1-7/+*; *pnh-2/pnh-2* mutant flowers develop filamentous organs in place of petals (Fig. 8A; Table 4). Such filaments are not seen in *pnh-2/pnh-2* flowers (Table 4). *ago1-7/+*; *pnh-2/pnh-2* mutant flowers also make more stamens and carpels than *pnh-2/pnh-2* flowers. This difference is statistically significant for carpels ($P < 0.01$). If petals and filaments are grouped together, *ago1-7/+*; *pnh-2/pnh-2* mutant flowers make more of this type of organ than *pnh-2* single mutants (Table 4). The short carpel defect is enhanced in *ago1-7/+*; *pnh-2/pnh-2* mutant flowers (Fig. 2F).

ago1-7/+; *pnh-2/pnh-2* mutants also show changes in leaf morphology. Cauline leaves are twisted, thickened and curled under at the margins, and, in extreme cases, are small and filamentous (Fig. 8C,D). In contrast to these effects, mutation in one copy of *AGO1* did not increase the frequency of empty axils (Table 3).

To analyze the phenotype of *ago1-7/ago1-7*; *pnh-2/+* plants, the *ago1* mutant self-progeny of *ago1-7/+*; *pnh-2/+* parents (group A) were compared to the *ago1* mutant self-progeny of *ago1-7/+* parents (group B). Two novel phenotypes were noted in group A. In flowers from about two-thirds (27/42) of *ago1* plants from group A, sepals are radialized and an ectopic growth forms internal to the fourth whorl carpels. This growth appears to be a central placenta with straight ovules developing from it (Fig. 8B). Rosette leaves also are affected. These appear

Fig. 8. *ago1* and *pnh* mutations have semi-dominant phenotypes in homozygous *pnh* and homozygous *ago1* backgrounds, respectively. (A) *ago1-7/+; pnh-2/pnh-2* flower. Arrow shows filamentous petal. (B) *ago1-7/ago1-7; pnh-2/+* flower. Arrow shows ovule developing from a central stalk. (C) *ago1-7/+; pnh-2/pnh-2* inflorescence stem and cauline leaves. Arrow points to filamentous organ on the secondary inflorescence. (D) Enlargement of a filamentous structure similar to that in C. (E) Cross section through wild-type rosette leaf. Adaxial is to the right. (F) Cross section through *ago1-7/ago1-7* rosette leaf. Adaxial is to the right. (G) Cross section through *ago1-7/ago1-7; pnh-2/+* rosette leaf. Orientation is unknown. c, carpel; p, phloem; x, xylem. Scale bar, 250 μ m (A,B) and 25 μ m (E-G).



radialized in about two-thirds of the *ago1* plants in group A (34/50) in contrast to the flattened rosette leaves in *ago1* single mutants. Internally, the normal polar organization of the vasculature is disrupted such that xylem, an adaxial cell type, is surrounded by phloem, an abaxial cell type (Fig. 8E,G). This arrangement is unaffected in the *ago1* single mutant rosette leaves (Fig. 8F).

Although no distinct phenotype was detected in double heterozygotes, the novel phenotypes seen in each homozygous mutant when one copy of the other gene is mutant indicate that both *PNH* and *AGO1* are partially able to compensate for a decrease in activity of the other gene. The synergistic effect of double mutations in *pnh* and *ago1* demonstrate that these genes have overlapping functions.

DISCUSSION

Hypotheses for the variable SAM phenotype of *pnh* mutants

The *PNH* gene is required for efficient SAM formation during embryogenesis. However, the *pnh* SAM defect is quite variable. Even in lines homozygous for what should be strong mutant alleles, a significant number of individuals form apparently normal meristems. We originally hypothesized that this variability was seen because the alleles we isolated were not null (McConnell and Barton, 1995). The molecular data make this hypothesis less likely and we now favor either of the following non-mutually exclusive hypotheses.

One hypothesis posits that the ability of some *pnh* embryos to form SAMs is due to the action of a redundant gene(s) that supplies *PNH*-like function. Based on several criteria, *AGO1* is a good candidate for such a redundant gene. The *AGO1* expression pattern overlaps that of *PNH*, mutations in either of the two genes cause similar SAM defects, the amino acid sequences are highly similar, and the double mutant demonstrates that these genes have overlapping functions. Neither *ago1* nor *pnh* mutations cause a fully penetrant SAM

formation defect on their own, and in both mutants STM protein accumulates in early stages of SAM formation. By contrast, double mutant embryos fail to accumulate detectable STM protein. According to this hypothesis, *PNH* would be involved in the earliest stages of SAM formation while the apparent ability of *pnh* mutants to proceed through early SAM formation is due to *AGO1* activity.

Alternatively, the *PNH* gene may be required for the proper placement of leaf primordia. In support of this idea, the expression of *PNH* in the presumptive leaf trace anticipates the production of p-1, a leaf primordium that previously has not been detectable within the meristem, even by the criterion of *STM* expression. In the absence of *PNH* function, leaves would form at random sites on the meristem. If a leaf forms at the meristem summit, the SAM is consumed in the production of the determinate organ. The SAM would be especially sensitive to termination during embryogenesis when it is small and much less susceptible to termination by this mechanism later in development when it is larger. According to this hypothesis, the failure of the double mutant to express the STM protein is due to other, more fundamental defects (see below).

Environmental factors also may play a role in determining the penetrance of the *pnh* mutation. In our previous study, plants were grown at a different location and the penetrance was significantly higher.

Role in postembryonic (axillary) meristem formation

In addition to its role in the embryo, *PNH* is required for the efficient formation of axillary meristems during postembryonic development. This is consistent with the persistent expression of *PNH* mRNA in the meristem and in the adaxial leaf domain. Our results differ from findings by Moussian et al. who reported that *PNH* expression in the SAM was limited to a short time late in embryogenesis. They also reported that failure to form axillary meristems was limited to secondary inflorescences and was secondary to fasciation. Thus, they concluded that *PNH* function was required specifically for

SAM formation in the embryo. We find no correlation between fasciation and failure to form axillary meristems.

As described in the introduction, several observations indicate that the adaxial leaf domain possesses a unique competence to form meristems. If a factor exists that is responsible for the competence of the adaxial leaf domain to make SAMs, we expect such a factor to be expressed or active preferentially in the adaxial side of the leaf and to cause defects in meristem formation when mutant. *PNH* satisfies both of these criteria and therefore is a candidate for such a hypothetical competence factor.

Given the experimental evidence for the association between adaxial leaf domain and meristem-forming competence, it is interesting that the adaxial leaf domain and SAM constitute a region of shared positional identity in the plant by the criterion of low-level *PNH* expression. This domain adds to our understanding of molecular prepatterns that exist in the SAM, especially along the radial axis. An interpretation of this expression pattern is that the SAM develops as a subdomain of the adaxial leaf in *Arabidopsis*.

Does *PNH* play a wider role in the development of central fates?

Given the relatively mild meristem formation defect in *pnh* mutants as compared to *stm* mutants, the early and extensive expression of *PNH* mRNA was surprising. In the embryo, *PNH* mRNA accumulation occurs in other cells as well as in the presumptive SAM and is found as early as the four-cell stage of embryogenesis. *PNH* expression is progressively restricted to more central regions suggesting that *PNH* plays a general role in the development of central fates. The occurrence of disorganized embryos in *pnh* lines and the phenotype of the double mutant shows that *PNH* (and *AGO*) is required early in the development of the embryo and for events other than SAM formation. If *PNH* has a role in the development of central fates, it does not appear to be required for specification of cell types because double mutants possess vascular, ground, and epidermal cell types in the appropriate layers. However cells within these layers – most notably in the vascular cylinder where *PNH* expression is highest – are highly disorganized compared to the wild type. Whether these genes play a role in establishing some specific aspect(s) of embryo development or whether they are required in a more general way for growth still is unknown.

Are *ago1* and/or *pnh* mutants altered in leaf polarity?

In a transverse section through the apex (diagram in Fig. 4C), it becomes clear that ad- and abaxial leaf domains of a presumptive leaf primordium are positions along the radial axis of the SAM. The restriction of *PNH* to adaxial cells of leaves suggests that *PNH* is required for some aspect of adaxial leaf development. As discussed above, this could be competence for meristem development. If competence to form meristems is indeed an adaxial trait, it is genetically separable from other, morphological adaxial traits because leaves of *pnh* mutants are anatomically normal. The exception to this is the leaves that develop in place of the meristem. These may be trumpet-shaped, with abaxial tissue on the outside of the bell (the opposite of adaxialized, *phb-1d* leaves) or they may be slender, apparently abaxialized, pin-like structures. The abaxialization

of these leaves could be due to a requirement for *PNH* in adaxial leaf development or to their aberrant positioning.

Interestingly, *AGO1*, the expression pattern of which is nearly ubiquitous in growing tissues, causes some transformation of adaxial to abaxial characters when mutated. This is most evident in the petal; other organs are less clearly abaxialized. Perhaps other members of the *PNH/AGO1* gene family function in the *ago1* mutant and prevent a complete transformation. *PNH* is a candidate for this, since in homozygous *ago1* mutants, mutation of one copy of *PNH* results in radialized rosette leaves and sepals.

Role of *PNH* in roots and vascular tissue

The expression pattern of *PNH* mRNA is puzzling. First, there is expression in the embryonic root meristem and in adult roots. Although the basal portion of the embryo sometimes is disrupted early in *pnh* embryogenesis, postembryonic root defects were not observed. Secondly, there is high-level expression in provascular tissue although examination of vascular tissues in *pnh* mutants showed only slight defects. Although *PNH*'s role in the vasculature is unclear, we can speculate that perhaps *PNH* is completely redundant to some other activity in these cells. Alternatively, vascular expression of *PNH* may be a source of positional information to which other tissues, like the SAM, respond. Finally, we may have missed subtle defects in these tissues.

AGO1/PNH gene family

The *AGO1/PNH* family of genes is found throughout all eukaryotic phyla (Bohmert et al., 1997; Moussian et al., 1998), including unicellular organisms such as the yeast *S. pombe*. Twenty homologues can be identified in the nearly complete sequence of the *C. elegans* genome. To date, no mutant phenotype has been associated with this family of proteins except in *Arabidopsis*. This is not surprising if these genes are redundant to one another as multiple mutations would be required to yield a phenotype. The similarity of the *PNH/AGO1* family of proteins to the rabbit translation initiation factor eIF2C raises the possibility that *PNH* and *AGO1* promote translation of mRNAs. It is also possible, however, that this family of proteins is involved in mediating protein-protein interactions in a variety of processes. eIF2C activity has been isolated from at least one plant, wheat (Osterhout et al., 1983; Seal et al., 1983), although the corresponding gene has not yet been identified.

Although it is premature to speculate on whether *PNH* and related sequences constitute a family of translation initiation factors, an exploration of the subject offers some ideas on how *PNH* may function. These proteins could play a general role in the translation of all mRNAs. However, the consistent viability, long life span, and the specificity of developmental defects seen in *pnh* and *ago1* single and double mutants argue against a general role in translation. Alternatively, *PNH* could promote translation of a specific subset of mRNAs. This subset might include such genes as *STM* and others required for meristem formation.

This work was supported by the National Science Foundation and the US Department of Agriculture; K. L. was supported by a fellowship from the National Science Foundation. We would like to acknowledge Heidi Barnhill for excellent assistance with scanning

electron microscopy. Thoughtful discussion and helpful comments on the manuscript were graciously contributed by Matt Evans, Jane McConnell and Scott Woody. We would like to thank Jane McConnell for providing the *ago1-8* allele, Alan Jones and Scott Poethig for the *pnh-9* allele and Yuval Eshed and John Bowman for the *pnh-10* and *pnh-11* alleles. This is paper number 3523 from the Laboratory of Genetics.

REFERENCES

- Barton, M. K. and Poethig, S.** (1993). Formation of the shoot apical meristem in *Arabidopsis thaliana*: an analysis of development in the wild type and in the shoot meristemless mutant. *Development* **119**, 823-831.
- Bohmert, K., Camus, I., Bellini, C., Bouchez, D., Caboche, M. and Benning, C.** (1997) *AGO1* defines a novel locus of *Arabidopsis* controlling leaf development. *EMBO J.* **17**, 170-180.
- Chuck, G., Lincoln, C. and Hake, S.** (1996). *KNAT1* induces lobed leaves with ectopic meristems when overexpressed in *Arabidopsis*. *Plant Cell* **8**, 1277-1289.
- Endrizzi, K., Moussian, B., Haecker, A., Levin J. Z. and Laux, T.** (1996). The *SHOOT MERISTEMLESS* gene is required for maintenance of undifferentiated cells in *Arabidopsis* shoot and floral meristems and acts at a different regulatory level than the meristem genes *WUSCHEL* and *ZWILLE*. *Plant J.* **10**, 967-979.
- Estruch, J. J., Prinsen, E., Onckelen, H. V., Schell, J. and Spena, A.** (1991). Viviparous leaves produced by somatic activation of an inactive cytokinin-synthesizing gene. *Science* **254**, 1364-1367.
- Evans, M. E. and Barton, M. K.** (1997). Genetics of angiosperm shoot apical meristem development. *Annu. Rev. Plant Physiol. Plant Mol. Biol.* **48**, 673-701.
- Furner, I. J. and Pumfrey, J. E.** (1992). Cell fate in the shoot apical meristem of *Arabidopsis thaliana*. *Development* **115**, 755-764.
- Irish, V. and Sussex, I. M.** (1992). A fate map of the *Arabidopsis* embryonic shoot apical meristem. *Development* **115**, 745-753.
- Long, J. A., Moan, E. I., Medford, J. and Barton, M. K.** (1996). A member of the KNOTTED class of homeodomain proteins encoded by the *SHOOTMERISTEMLESS* gene of *Arabidopsis*. *Nature* **379**, 66-69.
- McConnell, J. R. and Barton, M. K.** (1995). Effect of mutations in the *PINHEAD* gene of *Arabidopsis* on the formation of shoot apical meristems. *Dev. Genet.* **16**, 358-366.
- McConnell, J. R. and Barton, M. K.** (1998). Leaf polarity and meristem formation in *Arabidopsis*. *Development* **125**, 2935-2942.
- Moussian, B., Schoof, H., Haecker, A., Jurgens, G. and Laux, T.** (1998). Role of the *ZWILLE* gene in the regulation of central shoot meristem cell fate during *Arabidopsis* embryogenesis. *EMBO J.* **17**, 1799-1809.
- Osterhout, J. J., Lax, S. R. and Ravel, J. M.** (1983). Factors from wheat germ that enhance the activity of eukaryotic initiation factor eIF-2. *J. Biol. Chem.* **258**, 8285-8289.
- Perry, S. E., Nichols, K. W. and Fernandez, D. E.** (1996). The MADS domain protein AGL15 localizes to the nucleus during early stages of seed development. *The Plant Cell* **8**, 1977-1989.
- Seal, S. N., Schmidt, A. and Marcus, A.** (1983). Wheat germ eIF2 and CoeIF2. *J. Biol. Chem.* **258**, 10573-10576.
- Sinha, N., Williams, R. E. and Hake, S.** (1993). Overexpression of the maize homeobox gene, *Knotted-1*, causes a switch from determinate to indeterminate cell fates. *Genes Dev.* **7**, 878-795.
- Snow, M. and Snow, R.** (1942). The determination of axillary buds. *New Phytol.* **41**, 13-22.
- Talbert, P., Adler, H.-T., Parks, D. W. and Comai, L.** (1995). The *REVOLUTA* gene is necessary for apical meristem development and for limiting cell divisions in the leaves and stems of *Arabidopsis thaliana*. *Development* **121**, 2723-2735.
- Tsay, Y. F., Frank, M. J., Page, T., Dean, C. and Crawford, N. M.** (1993). Identification of a mobile endogenous transposon in *Arabidopsis thaliana*. *Science* **260**, 342-344.
- Zou, C., Zhang, Z., Wu, S. and Osterman, J. C.** (1998). Molecular cloning and characterization of a rabbit eIF2C protein. *Gene*, **211**, 187-194.